

Prasanna Karpur,<sup>1</sup> Theodore E. Matikas,<sup>2</sup> Mark P. Blodgett,<sup>3</sup>  
Jay R. Jira,<sup>4</sup> and Drew Blatt<sup>4</sup>

## Nondestructive Crack Size and Interfacial Degradation Evaluation in Metal Matrix Composites Using Ultrasonic Microscopy

---

**REFERENCE:** Karpur, P., Matikas, T. E., Blodgett, M. P., Jira, J. R., and Blatt, D., "Non-destructive Crack Size and Interfacial Degradation Evaluation in Metal Matrix Composites Using Ultrasonic Microscopy," *Special Applications and Advanced Techniques for Crack Size Determination, ASTM STP 1251*, J. J. Ruschau and J. K. Donald, Eds., American Society for Testing and Materials, Philadelphia, 1995, pp. 130-146.

**ABSTRACT:** Ultrasonic scanning acoustic microscopy is a nondestructive method useful for material elastic property quantification as well as crack size determination for surface and subsurface cracks. The advantage of the method over destructive methods for crack size determination is that the imaging technique can provide the crack sizing information while helping in the detection of interface degradation and early crack initiation so that their growth can be monitored during interrupted fatigue tests. Various metal matrix composite systems with titanium based matrix and SCS-6 fibers have been evaluated for this study [Ti-24Al-11Nb (atomic percent), Ti-6Al-2Sn-4Zr-2Mo (weight percent), and Ti-15Mo-3Nb-3Al-0.2Si (weight percent)]. The scanning acoustic microscope technique has been applied to materials subjected to both room temperature and elevated temperature fatigue cycling in addition to thermomechanical fatigue (in-phase and out-of-phase) conditions. A 50 MHz scanning acoustic microscope has been used for the imaging and evaluation of the damage initiation and growth of surface/subsurface cracks and interfacial degradation. All the images have been produced by exploiting the surface wave component of the ultrasonic signals from the scanning acoustic microscope because of the higher sensitivity of surface waves to both surface/subsurface cracks and perhaps also due to the changes in interfacial elastic properties. The results shown in this paper provide a very good understanding of the crack initiation and growth as well as interfacial degradation process of titanium based metal matrix composites when subjected to cyclical stresses at elevated temperatures and room temperature. The results indicate that the combination of high temperature and stress is very severe to the interface between the matrix and the fiber.

**KEYWORDS:** metal matrix composites, thermomechanical behavior, interfacial damage, non-destructive evaluation, ultrasound, scanning acoustic microscope, crack sizing, crack growth, crack initiation, Rayleigh waves, interfacial degradation, environmental effects

<sup>1</sup> Research Institute, University of Dayton, 300 College Park Avenue, Dayton, OH 45469-0127. Also, on-site contract, WL/MLLP, Materials Directorate, Wright Laboratory, Wright Patterson Air Force Base, OH 45433-7817. Contract number F33615-89-C-5612.

<sup>2</sup> National Research Council Associate, WL/MLLP, Materials Directorate, Wright Laboratory, Wright Patterson Air Force Base, OH 45433-7817.

<sup>3</sup> WL/MLLP, Materials Directorate, Wright Laboratory, Wright Patterson Air Force Base, OH 45433-7817.

<sup>4</sup> WL/MLLN, Materials Directorate, Wright Laboratory, Wright Patterson Air Force Base, OH 45433-7817.

Fiber reinforced composite materials are being considered for a number of applications because of their improved mechanical properties as compared to nonreinforced materials. In applications where cyclic loading is expected and where life management is required, consideration must be given to the behavior of the material in the vicinity of stress risers such as notches and holes. It is in these regions that damage initiation and accumulations are expected. In the case of metal matrix composites for aircraft structural and engine components, several damage modes near stress risers have been identified [1]. One important damage mode under cyclic loading is the nucleation and growth of matrix cracks perpendicular to the fiber direction. In some composite systems, the matrix crack growth occurs without the corresponding failure of the fibers. This process results in the development of relatively large matrix cracks that are either fully or partially bridged by unbroken fibers. The presence of bridging fibers can significantly influence the fatigue crack growth behavior of the composite. To develop a life prediction methodology applicable to these composite systems, an understanding must be developed of both the matrix cracking behavior as well as the influence of the unbroken fibers on the crack driving force and the affect of interfacial degradation and damage on the eventual failure of the composite.

Paramount to understanding the influence of unbroken fibers is understanding the mechanisms which transfer the load from the matrix to the fiber. The mechanics of matrix cracking and fiber bridging in brittle matrix composites has been addressed [2,3]. The analysis is based on the shear lag model to describe the transfer of load from the fiber to the matrix. In the shear lag model, the transfer of load occurs through the frictional shear force ( $\tau$ ) between the fiber and the matrix. The analyses indicate that size of the region on the fiber over which  $\tau$  acts can have a significant effect on the influence of unbroken fibers on crack growth rate behavior. However, although some indirect ultrasonic experimental techniques have been developed to determine the extent of the influence of  $\tau$  [4-6], no direct nondestructive experimental techniques have been demonstrated to determine the extent of the influence of  $\tau$ . Another important interfacial phenomenon is the degradation, fracture, or failure of the interface resulting from crack initiation and growth which is the aspect of interest in this paper.

The objective of this paper is to demonstrate the utility and versatility of scanning acoustic microscopy (SAM) for material behavior research of metal matrix composites. Hence, in the work reported in this paper, the SAM technique is utilized for nondestructively determining regions of interfacial degradation while simultaneously providing indications of surface crack length in three metal matrix composite systems. The specimens have been subjected to various test conditions including room temperature, isothermal mechanical fatigue, and thermomechanical fatigue. In the interfacial regions of all the specimens, subsequent destructive evaluations are used to verify the indications revealed by SAM.

### Scanning Acoustic Microscopy (SAM)

Scanning acoustic microscopy was developed by Quate et al. [7,8]. It has been extensively studied by Briggs et al. [9-13] since that time. The most important contrast phenomenon in a SAM is the presence of Rayleigh waves which are leaking toward the transducer and are very sensitive to local mechanical properties of the materials being evaluated. The generation and propagation of the leaky Rayleigh waves are modulated by the material properties, thereby making it feasible to image even very subtle changes of the mechanical properties.

A SAM transducer is schematically shown in Fig. 1. The transducer has a piezoelectric active element situated behind a delay line made of silica crystal oriented such that the 1-1-1 axis is parallel to the direction of sound propagation. The thickness of the active

element is suitable to excite ultrasonic signals (with a nominal frequency of 50 MHz in this case) when an electrical spike voltage is delivered to the piezoelectric element. The silica delay has a spherical acoustical concave lens (Fig. 1) which is ground to an optical finish. The numerical aperture (NA, ratio of the diameter of the lens to the focal distance) is 1.25 for the transducer used for this study. An NA of more than 1 (or F number, focal distance/diameter, of the lens less than 1) is essential for the SAM technique to effectively generate and receive surface waves in the specimen being imaged.

The principle of operation of a SAM transducer is based on the production and propagation of surface acoustic waves (SAW) as a direct result of a combination of the high curvature of the focusing lens of the transducer and the defocus of the transducer into the specimen [7,14]. The contrast of the images obtained using SAM is based on the attenuation and

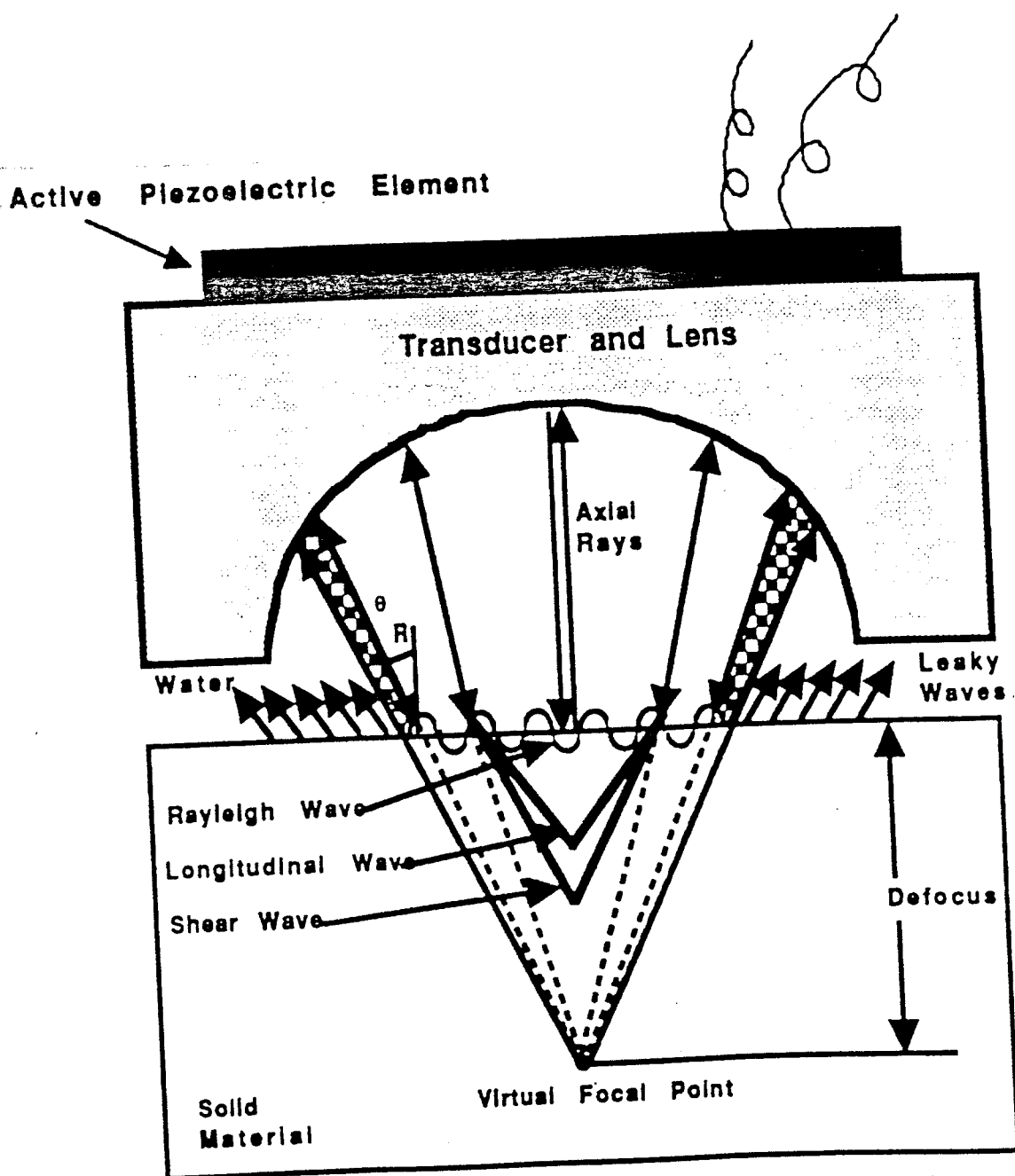


FIG. 1—Schematic of a SAM. The diagram shows the active piezo electric element, focusing lens, and the Rayleigh wave generated due to the sharp focusing of the ultrasonic beam.

reflection of SAW. In addition, the sensitivity of the SAW signals to the surface and the subsurface features depend on the degree of defocus and has been well documented in the literature as the  $V(z)$  curves [15]. The defocus distance also has another important effect on the SAW signal obtained by the SAM transducer: the degree of defocus dictates whether the SAW signal is well separated from the specular reflection or interferes with it. Thus, depending on the defocus, the SAM technique can be used either to map the interference phenomenon in the first layer of subsurface fibers or to map the surface and subsurface features (reflectors) in the specimen.

### Test Specimens

The SAM was used in conjunction with several on-going material behavior investigations [16-18] to evaluate the extent of damage accumulated during the respective test procedures. Specimens were removed during or after testing and evaluated using the SAM. Thus, composite materials composed of a range of different matrix materials could be evaluated. All the specimens are titanium matrix composites reinforced with a silicon-carbide based fiber, commercially designated SCS-6, that has a double pass carbon rich coating. The matrix materials include a beta processed titanium alloy, Ti-15Mo-3Nb-3Al-0.2Si (weight percent: Specimens 1, 2, and 3), a conventional titanium alloy Ti-6Al-2Sn-4Zr-2Mo (weight percent: Specimen 4), and an alpha-two titanium aluminide alloy, Ti-24Al-11Nb (atomic percent: Specimen 5). The Ti-24Al-11Nb and Ti-15Mo-3Nb-3Al-0.2Si composites were manufactured using the foil-fiber-foil process, and the Ti-6Al-2Sn-4Zr-2Mo was manufactured using the plasma spray technique.

### Experimental Configuration

The ultrasonic imaging was done by using a 50 MHz nominal frequency SAM transducer with a focal spot size of approximately 15  $\mu\text{m}$  (theoretical) when focused on the surface of the specimen. The ultrasonic beam was defocused into the specimens to generate leaky Rayleigh waves propagating along the surface. The defocus was enough to avoid interference of the surface wave with the specular reflection from the front surface of the specimen (the exact defocus distance for each specimen to generate and receive leaky Rayleigh waves, however, is dependent on the properties of the matrix material). The depth of penetration of 50 MHz surface waves is about 140  $\mu\text{m}$  (theoretical). The SAM transducer was raster scanned in a plane parallel to the surface of the specimen while simultaneously producing and receiving Rayleigh waves. The digitally recorded Rayleigh wave signals were software gated [19], and the resulting amplitude was plotted to generate the acoustic micrographs shown in this paper.

### Results

The results of SAM applied to metal matrix composites (MMC's) will be presented under several subsections based on the type of composite system being imaged. The fatigue test parameters for each specimen will be outlined for each specimen in the corresponding subsections.

#### *Specimen 1: SCS-6/Ti-15Mo-3Nb-3Al-0.2Si*

One benefit of the SAM is that it provides a nondestructive indication of the extent of interfacial damage. To demonstrate its utility, a notch (hole) fatigue experiment was peri-

odically interrupted and the specimen was scanned using the SAM to evaluate the development of damage during the life of the specimen. After each SAM evaluation, the specimen was returned for further fatigue cycling. The fatigue cycling was terminated after the third interruption at  $9.66 \times 10^5$  cycles. For this test, the composite consisted of a cross-ply layup of fibers in the [0/90]<sub>n</sub> configuration. Prior to testing, a SAM image was made of the specimen to establish the initial integrity of the material. The pretesting image is shown in Fig. 2a and shows no damage to the interfaces prior to testing.

After the initial scan, the specimen was fatigued isothermally at 650°C with a maximum remote stress of 200 MPa applied at 1 Hz along the fibers with reference to the image in Fig. 2a. The fatigue test was stopped after  $1.54 \times 10^5$  cycles or approximately 43 h at the specified high temperature. One matrix crack could be seen on each side of the hole. One

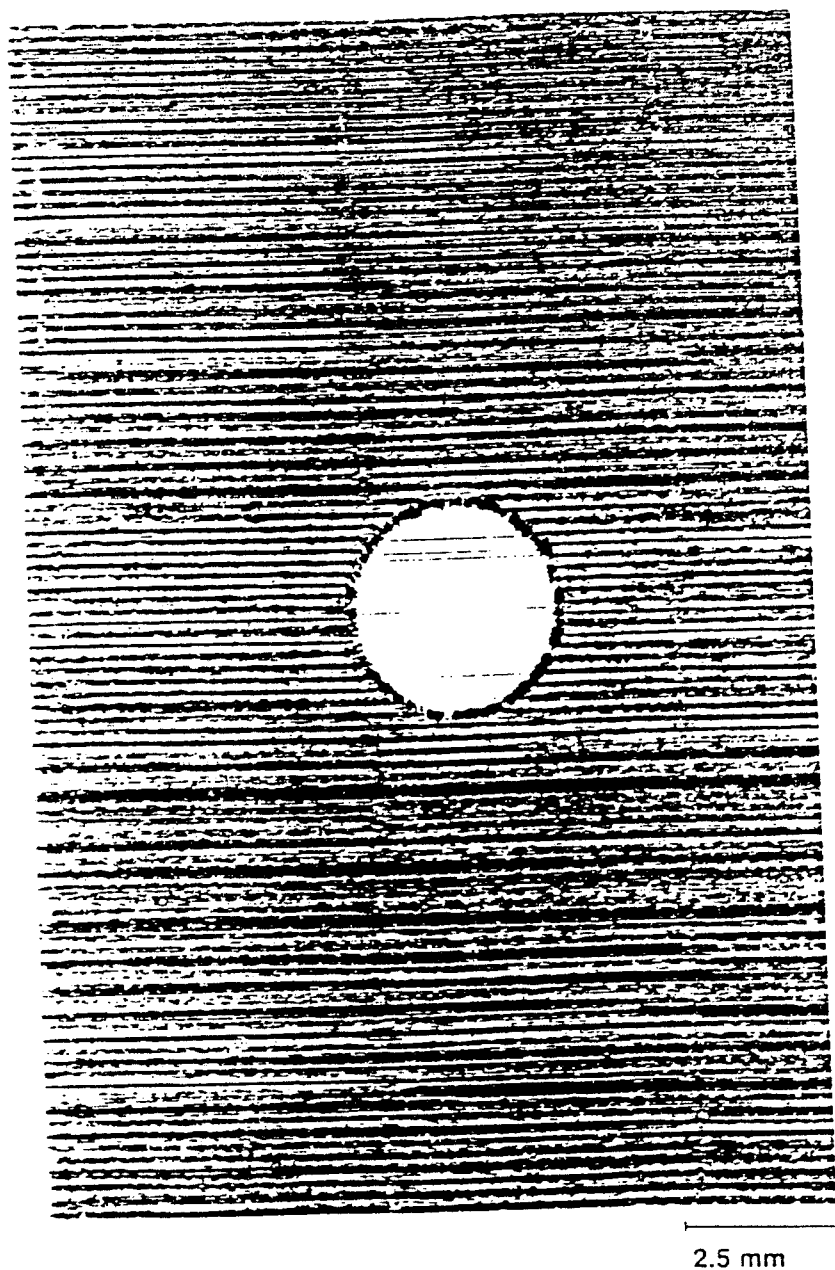


FIG. 2a—The SAM image of a Ti-15Mo-3Nb-3Al-0.2Si (weight percent) specimen before an isothermal (650°C) fatigue test.

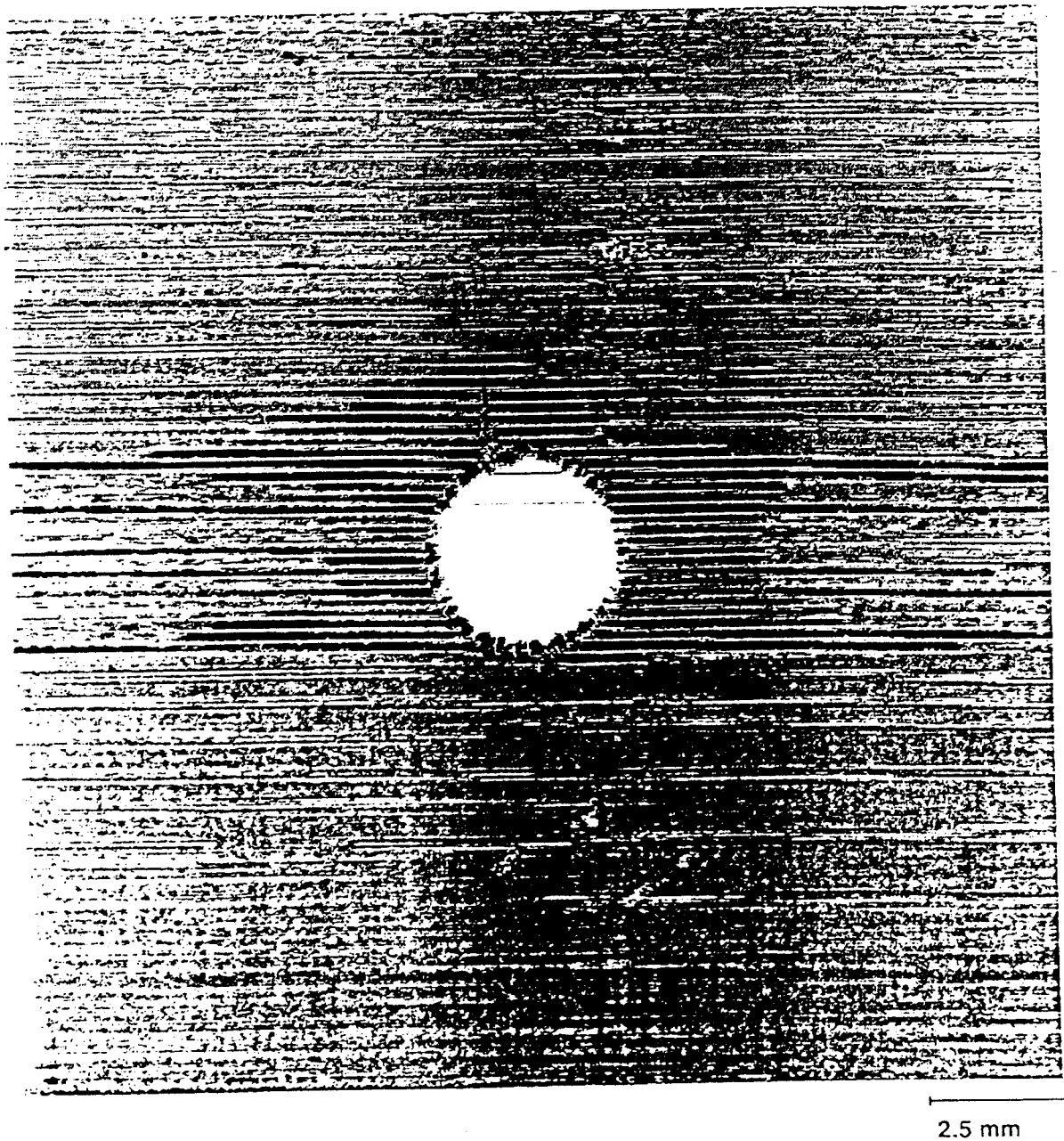


FIG. 2b—The SAM image of the Ti-15Mo-3Nb-3Al-0.2Si (weight percent) specimen in Fig. 2a after  $1.54 \times 10^7$  cycles or approximately 43 h of isothermal (650°C) fatigue test.

crack initiated earlier in the test and had a surface length of 2.36 mm from the edge of the hole while the crack on the other side had reached a length of 0.54 mm from the edge of the hole. The specimen was removed from testing and imaged using the SAM. The resulting image is shown in Fig. 2b. In this figure, the damage (as indicated by the high contrast regions) originates at the top and bottom of the hole and proceeds away from the hole along the fibers. The damage is also seen to originate at the crack plane, where the crack exposes the interior of the specimen to the environment. The actual crack length is longer than the length over which the high contrast region is observed. This difference corresponds to approximately three fibers at each crack tip and appears to be related to the relatively recent extension of the crack into this region and perhaps the consequential shorter duration over

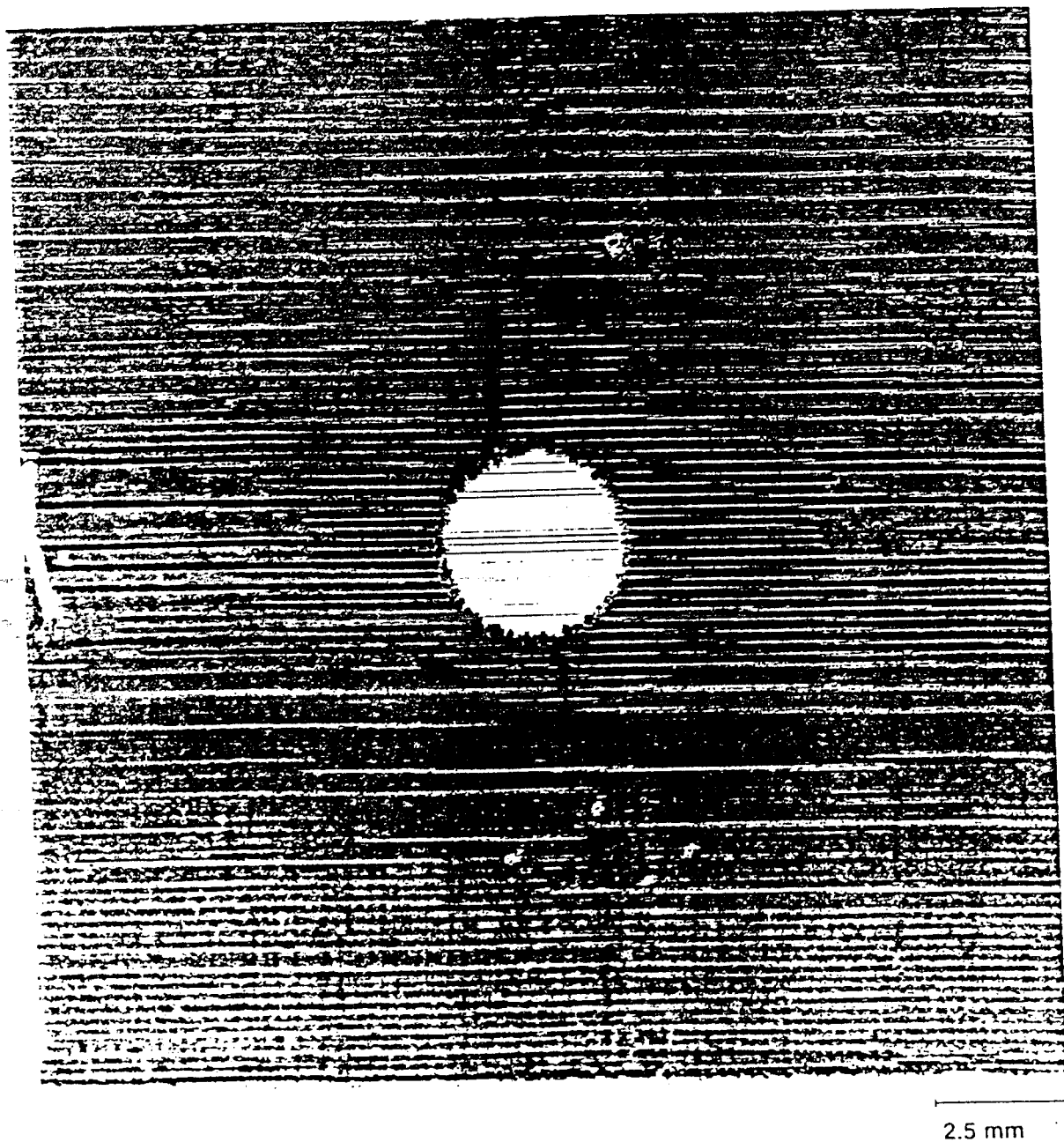


FIG. 2c—The SAM image of the Ti-15Mo-3Nb-3Al-0.2Si (weight percent) specimen in Fig. 2a after  $2.51 \times 10^6$  cycles or approximately 70 h of isothermal (160°C) fatigue test.

which the environment has had access to those fiber-matrix interfaces. The shorter crack on one side of the hole is only beginning to develop an affected zone and is barely visible in the ultrasonic image although the crack extends about three fiber diameters at the surface.

Figure 2c is the SAM image after an additional  $9.66 \times 10^4$  cycles were applied for a total of  $2.51 \times 10^6$  cycles and total time of 70 h at the specified high temperature. In this figure, the cracks on each side of the hole can be seen clearly. The larger crack had grown to a surface length of 2.88 mm from the edge of the hole while the crack on the other side had reached a length of 1.77 mm from the edge of the hole. The region of high contrast has expanded along the cracks as well as to the left and right of the hole. However, in the SAM

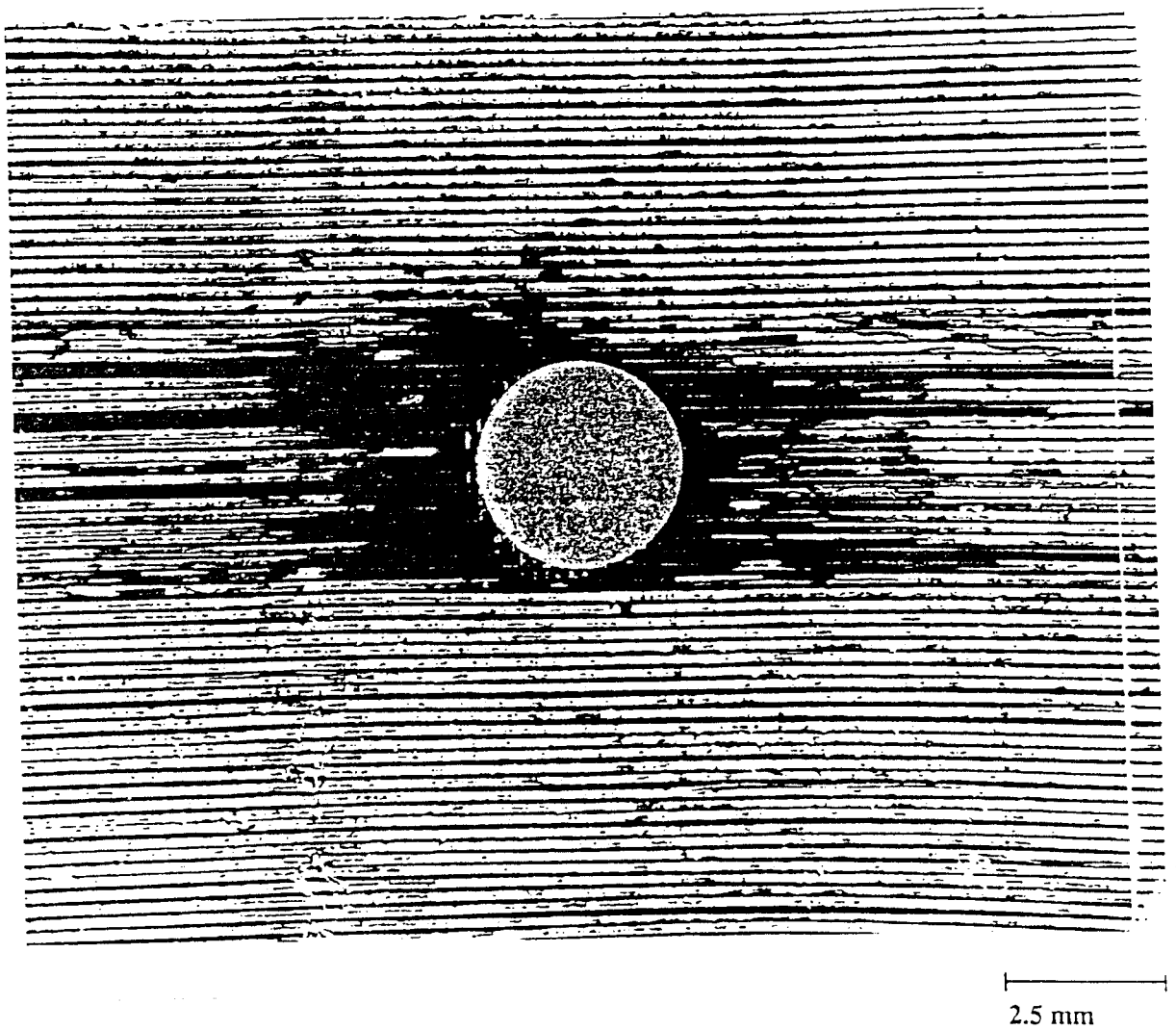


FIG. 2d—Metallography of specimen in Fig. 2a through 2c.

image in Fig. 2c, the last three fibers at the tips of both the cracks did not show any interfacial damage.

To substantiate the indications made by the SAM, the outer layer of matrix material on Specimen 1 was etched away using a saturated solution of tartaric acid in 10% bromine in methanol. The etched specimen was cleaned ultrasonically in acetone, photographed, and is shown in Fig. 2d. Throughout most of the exposed layer of fibers, the outer coatings of the fibers have remained intact and appear white. The dark regions above and below the hole indicate the cracking of the coating. In most cases, when the environmental exposure time is maximum, the coatings have been removed completely, exposing the dark silicon carbide fibers beneath the coating. The cross-ply ( $90^\circ$ ) fibers in the second layer can also be detected. From the metallographic image in Fig. 2d, the hypothesis of gradual degradation of the interface is suggested because the interfaces of the fibers cut by the circumference of the hole were exposed the longest to the severe environmental conditions and show enough damage to lose the interfacial coating during cleaning. However, the longer and older of the two cracks show some damage to the interface whereas the shorter crack shows almost no damage in the metallography although ultrasonic images indicate otherwise. Plans are un-

derway to conduct elevated temperature experiments in inert atmosphere to further evaluate the effect of oxygen on the interfacial degradation process.

*Specimen 2: SCS-6/Ti-15Mo-3Nb-3Al-0.2Si*

Specimen 2 is a four-ply, unidirectionally reinforced composite of SCS-6 fibers in Ti-15Mo-3Nb-3Al-0.2Si matrix. This beta processed matrix material was chosen for composite applications because of its improved environmental resistance at high temperatures. As such, Specimen 2 was fatigued at an elevated temperature (650°C) to investigate the notch and fatigue crack growth behavior of this composite system. The specimen was rectangular in shape with a width of 19 mm, length of 150 mm, and had a 4.76 mm diameter hole machined in the center. The fatigue loading was applied to the specimen in the direction of the fibers at a frequency of 1 Hz and at a maximum remote applied stress of 350 MPa. Fatigue cracks initiated quickly in the circular hole and grew until the specimen fractured after  $1.82 \times 10^5$  cycles. This corresponded to approximately 50 h of high temperature exposure during the life of this specimen. After testing, the specimen was evaluated using the SAM.

Figure 3 is a SAM image of Specimen 2. The fractured edge of the specimen including the remaining portion of the circular hole is on the right-hand side of the figure. Four cracks initiated around the hole, with one crack on each side of the hole dominating and eventually leading to failure. One of the nonfailure cracks, labeled E, is visible in Fig. 3. Note that the fiber locations are easily distinguished throughout the SAM image.

A region of high contrast, evident in Fig. 3, appears to extend along the fibers. The shape of the high contrast regions suggest that both the local stresses and the duration of exposure to the high temperature environment influence the extent of damage. The zones labeled A and B on the figure are regions of stress concentration near the notch. Cracks initiated in this region, exposing the interior of these regions to the environment early in the fatigue life. Consequently, the largest affected length of fibers appear to originate near A and B. In contrast, the affected fiber length between G and H is considerably less, even though the fiber ends at the hole were exposed to the environment from the beginning of the test. The geometry of the notch leads to fiber stresses in this region which are considerably smaller in magnitude than the stresses near A and B. It appears that the different stress state in this region has affected the rate of environmental interaction. The zones beginning at labels C and D and extending to each edge of the specimen are the regions of fast-fracture. In this region, the SAM did not detect strong differences from the virgin material. Finally, in the crack growth region shown by CA, BE, and BD, a gradient of affected fiber lengths is evident, presumably related to the duration of exposure after matrix cracking. These observations indicate that the effect detected by the SAM is related to both stress and exposure duration.

*Specimen 3: SCS-6/Ti-15Mo-3Nb-3Al-0.2Si*

A thermomechanical fatigue (TMF) crack growth test was conducted on a four-ply unidirectional composite with a titanium matrix reinforced with silicon-carbide, SCS-6, fibers [18]. The crack was grown perpendicular to the fiber and loading direction. The single-edge notch (SE(T)) specimen with clamped ends [20], was 25.37 mm wide and 0.96 mm thick with the initial EDM notch length equal to 7.593 mm. The specimen was subjected to a constant  $P_{max}$  throughout the test of 3.3 kN at an  $R$  (stress ratio  $R = s_{min}/s_{max}$ ) of 0.1 out-of-phase with a thermal cycle between 150 and 538°C. Out-of-phase means that the maximum load and minimum temperature occur at the same time during each cycle. The specimen

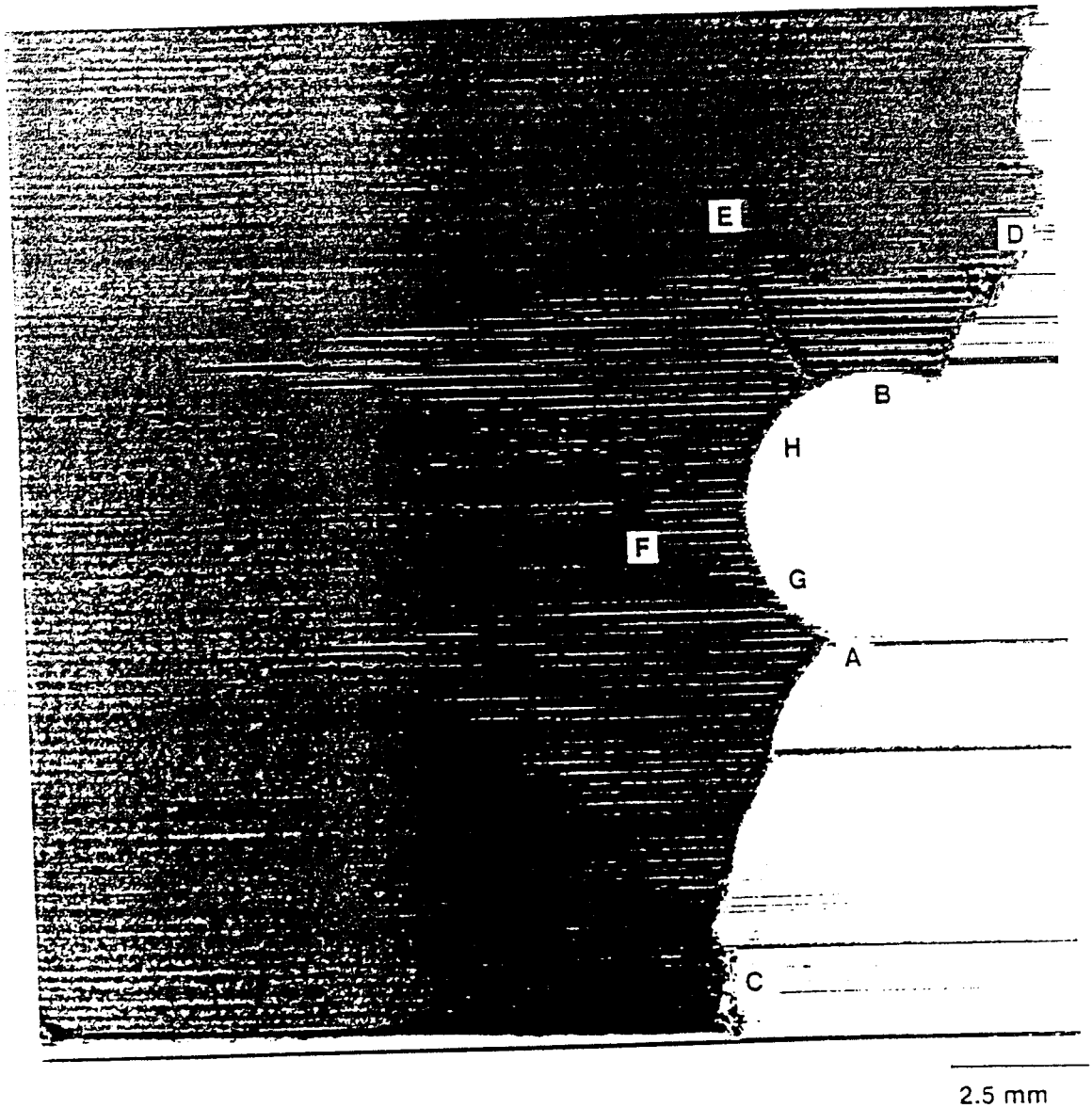
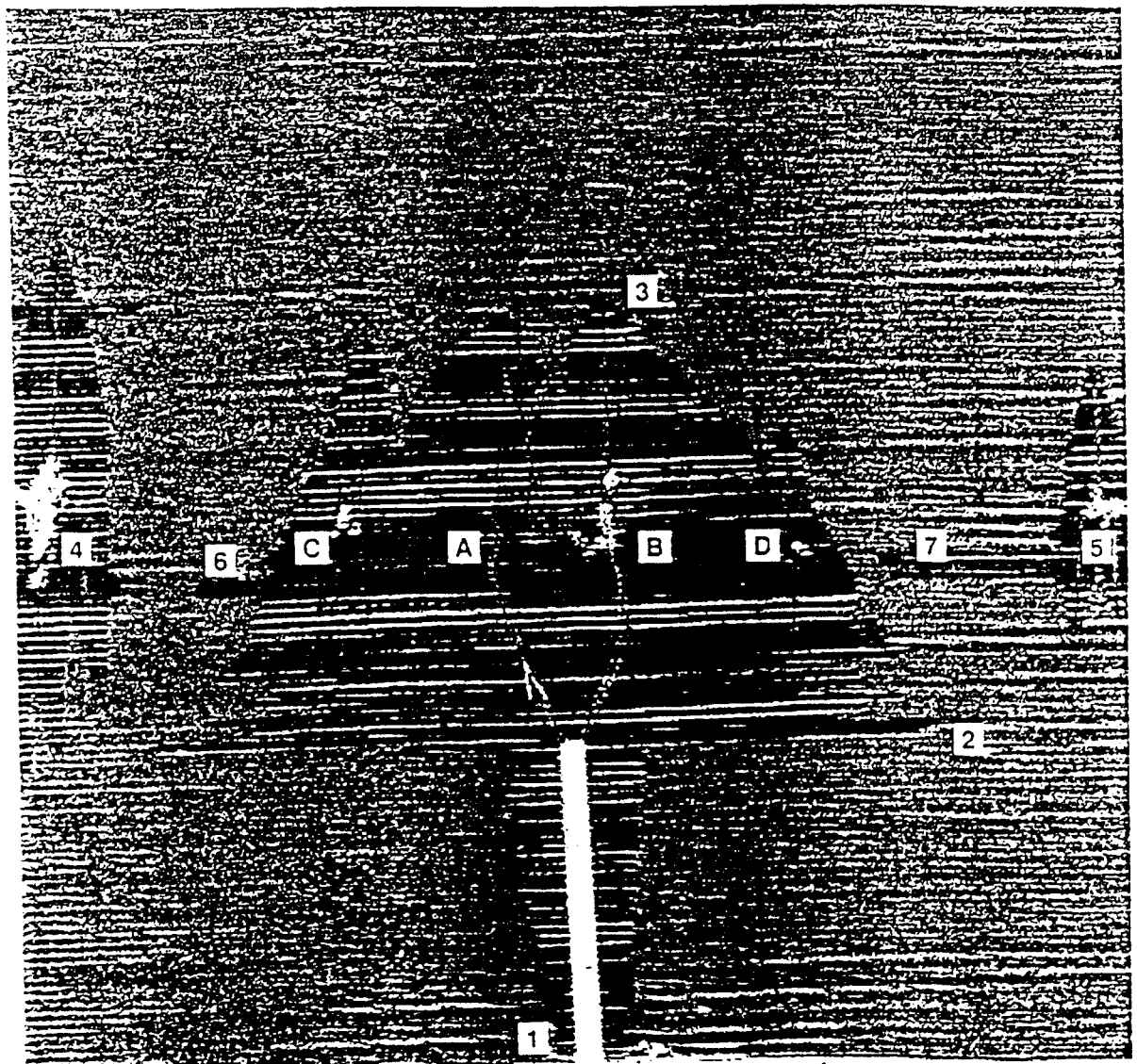


FIG. 3—The SAM image of a Ti-15Mo-3Nb-3Al-0.2Si (weight percent) specimen after an isothermal (650°C) fatigue test ( $1.82 \times 10^5$  cycles).

was subjected to 14 612 thermomechanical cycles over 36 days (0.0056 Hz). Further details of the test configuration can be found in the literature [18].

The first indication of the presence of an extensive zone of damage associated with the dominant matrix cracks was evidenced by a conventional "glass reflector plate" C-scan of the specimen [18]. Glass reflector plate technique [21] is a global method and provides the accumulated macro-damage in the entire thickness of the specimen. A well-defined damage zone was seen in the C-scan and prompted a further micro-evaluation of the area using SAM. Figure 4a shows the SAM image of the specimen. The image clearly shows the two dominant cracks, A and B (also visible on the surface to the naked eyes), growing from the tip of the notch. However, the ultrasonic SAM image shows a host of other features which provide invaluable information about the elevated temperature behavior as well as the degradation and failure mechanisms due to the combination of elevated temperature, applied stresses, presence of oxygen, and the duration of exposure.

The effects of the stress, temperature, and duration of exposure to elevated temperature can be seen clearly in Fig. 4a. The image is labeled to show seven zones, 1 through 7. Also, cracks are labeled A through D. In zone 1, where the effect of stress is gradually increasing toward the notch tip, the interface shows corresponding increasing lengths of degradation. The interfacial degradation and damage at the tip of the notch (zone 2) show a sudden increased length indicating that the stress in the first continuous fiber and the total time of exposure to elevated temperature have a devastating combined effect on the integrity of the interface. At zone 3 where the matrix crack tip is growing, the pointed shape of the interfacial oxidation followed by "parabolic" growth of the damage profile indicates that at the crack tip, the interfacial damage is not instantaneous. Zones 4 and 5 are cracks growing from the site of spot welds used to secure thermocouples. The zones show similar crack and interfacial damage mechanism as zones 1, 2, and 3. In addition, the areas labeled 6 and 7 on Fig. 4a show the process where interfacial damage from zone 4 as well as zone 5 are



2.5 mm

FIG. 4a—The SAM image of a Fe-15Mo-3Nb-3Al-0.2Si (weight percent) specimen after the specimen was exposed to 14 612 thermomechanical cycles over 36 days (0.0056 Hz).

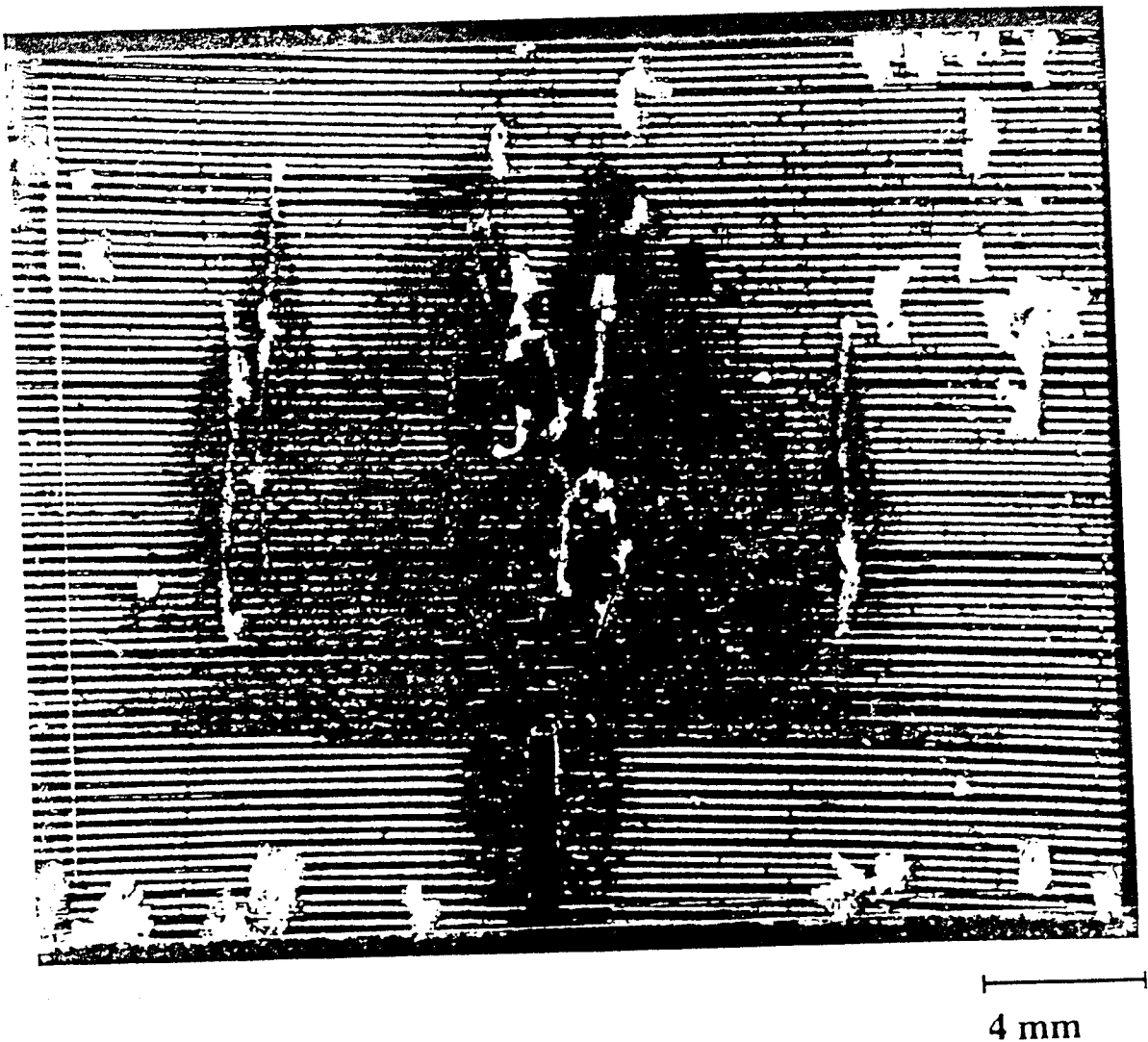


FIG. 4b—Metallography of specimen in Fig. 4a.

approaching the interfacial damage from cracks A, B, C, and D (C and D are cracks growing from unintentional weld spots on the surface). This behavior indicates that similar growth and merging behavior around cracks A, B, C, and D has resulted in the large mushroom shaped interfacial degradation and damage zone around the slot and the cracks.

Following the same procedure used for Specimen 1, the matrix was etched away to expose the first layer of fibers that were scanned (Fig. 4b). The photomicrograph in Fig. 4b shows a high degree of correlation with the SAM image. An examination of the etched specimen under the optical microscope revealed that the first layer of fibers showed a pattern of darkened fiber coatings that exactly matched the ultrasonic signature from the SAM. Closer inspection of the fiber coatings under a scanning microscope showed severe coating spalling in the darkened region. The coatings in the unaffected zone showed little damage, and what damage was visible was thought to be caused by the etching solution. The same effect of stress in the continuous fibers on the extent of damage was similar to that found in Specimens 1 and 2. The extent of fiber coating damage was greatly increased where the fibers were continuous (load carrying) and exposed to the environment due to matrix cracking. The stress-free fiber ends along the notch exhibited much less environmentally assisted damage along the fiber-matrix interface than the load carrying fibers left in the wake of the advancing

crack tip. It is important to note here that, at termination of the experiment, the crack tip was growing at a rate of approximately 0.1 mm during every 6 days. Thus, most of the interfacial degradation imaged by SAM is also seen by metallography, perhaps because of the extended duration of environmental exposure due to the slow crack growth rate of about 0.00069 mm/h.

*Specimen 4: SCS-6/Ti-6Al-2Sn-4Zr-2Mo*

A TMF crack growth test was conducted [22] on a four-ply unidirectional composite of Ti-6Al-2Sn-4Zr-2Mo matrix reinforced with silicon-carbide, SCS-6, fibers. The crack was grown perpendicular to the fiber and loading direction. The specimen, a single-edge notch (SE(T)) with clamped ends [20], was 25.07 mm wide and 0.83 mm thick with the initial EDM notch length equal to 7.481 mm. The specimen was subjected to a constant  $P_{max}$  throughout the test of 4.0 kN at an  $R$  of 0.1 in-phase with a thermal cycle between 150 and 538°C. In-phase means that the maximum load and maximum temperature occur at the same time during each cycle. The test frequency was 0.00833 Hz.

Figure 5 shows the SAM image of the specimen after 35 733 cycles were applied. The image clearly shows the two cracks, which are also visible to the naked eye, growing from the tip of the notch. Each crack has an average projected crack length of 8.9 mm. The distinct ultrasonic feature (dark areas) evident around the EDM notch and to a greater extent around the cracks indicates possible environment degradation of the carbon rich fiber-matrix

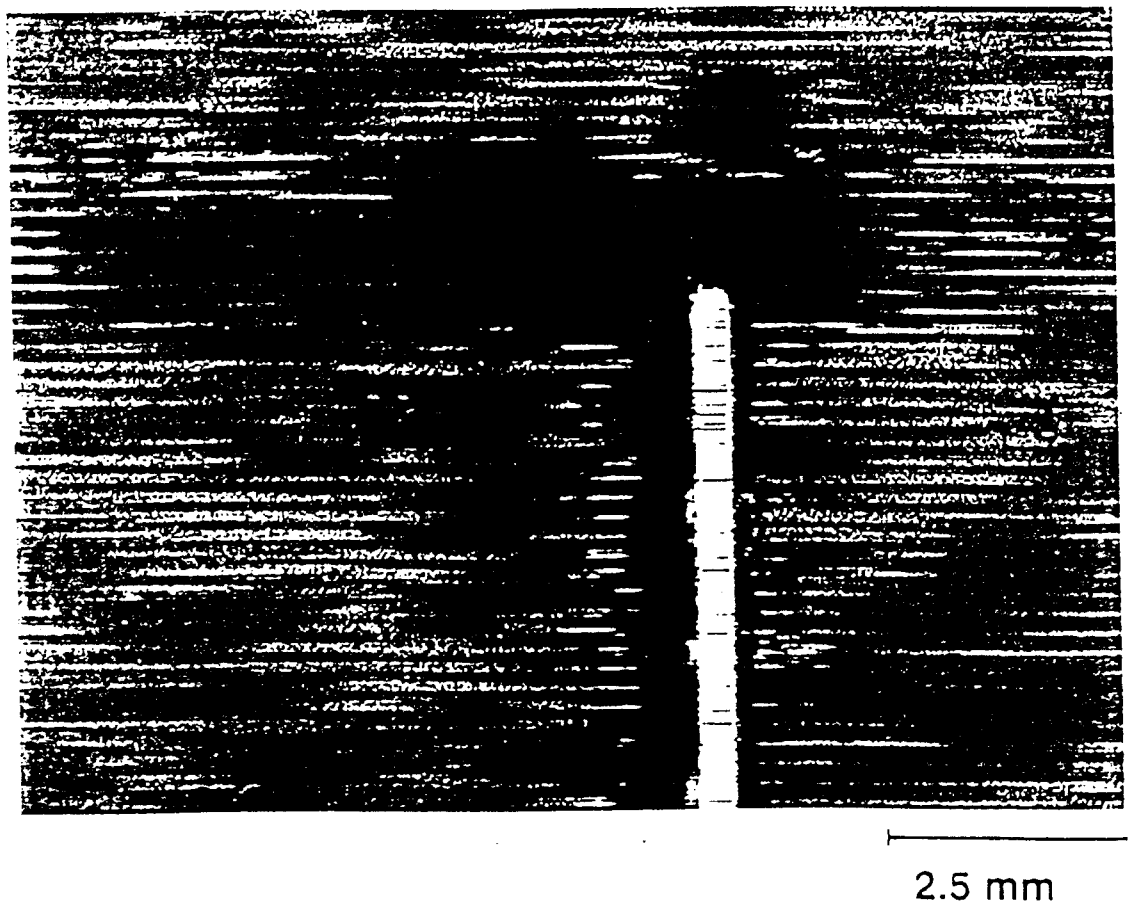


FIG. 5—The SAM image of a SCS-6/Ti-6Al-2Sn-4Zr-2Mo specimen after 35 733 cycles at 0.00833 Hz.

interfacial region. To confirm this, the matrix was etched away using a saturated solution of tartaric acid in 10% bromine in methanol. A visual inspection of the first layer of fibers after matrix removal showed a pattern of darkened fiber coatings that exactly matched the ultrasonic signature from the SAM.

#### *Specimen 5: SCS-6/Ti-24Al-11Nb*

In a recent investigation [16], the initiation and fatigue crack growth rates of cracks emanating from circular holes were investigated in an eight-ply, unidirectional layup of SCS-6/Ti-24Al-11Nb. Constant amplitude fatigue crack growth tests were conducted at a wide range of stress levels at a constant  $R$  equal to 0.1. In the investigation, it was found that cracks initiate at four locations around the hole very early in the fatigue life. Crack bridging by unbroken fibers was found to dominate the fatigue crack growth life as evidenced by the characteristic decrease in crack growth rates as the crack length increased during fatigue cycling. The SAM technique was applied to a specimen from this investigation to observe the matrix damage and evaluate the characteristics of a fully bridged matrix crack. The specimen was rectangular in shape with a width of 12.5 mm, length of 150 mm, and had a 3.2 mm diameter hole machined in the center. They were subjected to  $1.01 \times 10^5$  cycles at a maximum remote applied stress of 580 MPa at a frequency of 1 Hz. The fatigue loading direction was in the direction of the fibers with reference to Fig. 6.

Figure 6 shows the SAM image of a typical specimen after fatigue cycling at room temperature. It is clear from the figure that the primary cracks grew radially from the notch but turned to follow a direction perpendicular to the loading axis within a distance of one radius of the hole. Some secondary cracking can be seen near the primary cracks although these cracks formed later in the fatigue life and did not appear to participate in the final fracture. The locations of the fibers in the first layer can be seen easily as well as the location of a crossweave binder material used to hold the fibers in place during consolidation.

#### Discussion

The results from SAM imaging as well as metallography of Specimens 1 through 5 provide some very interesting and intriguing insight into the behavior and failure mechanisms of titanium based metal matrix composites with SCS-6 fibers. The results indicate, especially at elevated temperatures, that a chain of events occurs leading to eventual failure of the composites. The various events and the mechanisms observed will be discussed further with reference to each specimen tested and evaluated here.

The invaluable information that can be obtained from SAM in specimens tested at elevated temperatures is demonstrated clearly in Figs. 2 to 5. The interfacial degradation and damage evident in Fig. 2c, Fig. 3, Fig. 4a, and Fig. 5 were also corroborated by metallography. It is evident from the combination of SAM image and metallography that the extent of fiber coating damage was greatly increased where the fibers were continuous (load carrying) and exposed to the environment due to matrix cracking. The fiber ends exposed along the notch did accumulate some damage along the fiber-matrix interface but to a much lesser extent because they were in a stress free condition. This phenomenon in combination with larger damage near high stress areas such as the notch tips and hole circumference indicates that (1) when the stresses are negligible at the edge of the specimen, the interfacial degradation and damage is minimum even though the fiber/matrix interface was exposed to the temperature cycling during the entire duration of testing, and (2) the interfacial degradation is related directly to the fiber and matrix stresses which increase near the notch tip.

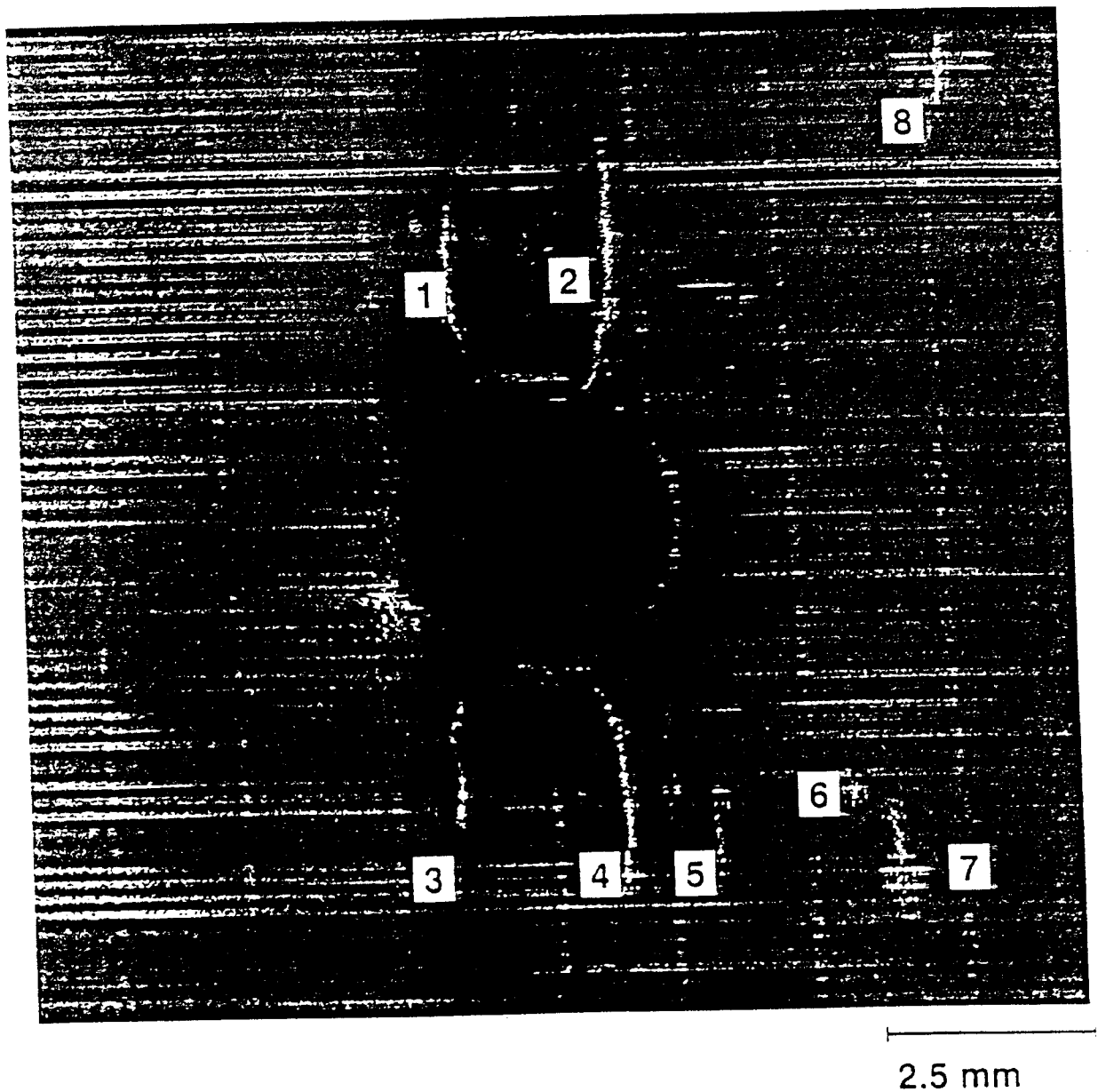


FIG. 6—The SAM image of a SCS-6/Ti-24Al-11Nb (atomic percent) specimen after room temperature.

It is apparent from the results that the crack tip merely provides access for environmental damage to attack the interface and that ahead of the crack tip no noticeable environmental damage occurs. Once the interface is exposed to the environment of elevated temperature and stresses, the interfacial degradation proceeds as indicated by the boundaries of the interfacial damage behind the crack tip. Thus, the relative size of the affected regions indicates that the extent of damage is related to the magnitude of the local stress level and the duration of exposure to elevated temperature. The stress level dependence is indicated by the relative size of the affected zones at the edge of the notch (a high stress region) when compared to the size at the top of the hole (a relatively low stress region). The time dependence is evidenced by a region near the crack tip where no fiber damage is indicated by the SAM. In this region, where the crack growth has occurred most recently, insufficient time has passed for the environment to be detrimental. Fibers which have been exposed to the environment later in life by the advance of the crack are affected less than fibers which were

The utility of SAM for the assessment of room temperature fatigue behavior of SCS-6/Ti-24Al-11Nb composite can be seen from Fig. 6. The SAM technique can easily detect primary cracking in the composite which normally can also be easily observed visually on the surface. However, the SAM also detects the presence of secondary cracking which is not always as evident as the primary cracks.

### Conclusions

Scanning acoustic microscopy has been shown to provide an invaluable insight into the fatigue crack growth behavior of titanium based metal matrix composites with SCS-6 fibers. The elastic waves produced by the SAM transducer are very sensitive to the local changes in elastic properties of the interfacial region. As a result, the technique is capable of detecting the onset of and monitoring the growth of interfacial damage, especially at elevated temperature.

The behavior of titanium based MMC's with SCS-6 fibers at both room temperature and elevated temperature has been analyzed in this study by conducting SAM analysis at room temperature. The results obtained from both SAM and metallography have provided invaluable information regarding the initiation and progress of interfacial damage. It has been found that the initiation of matrix cracking provides the necessary passage for the environment to reach the interfacial region. However, it has been shown that the environmental access alone is not sufficient for an accelerated interfacial degradation because it appears from the specimens in this study that temperature, stress, and duration of exposure are the three necessary factors for the degradation phenomenon to progress to maturity when most of the exposed interfacial region will be damaged.

### Acknowledgment

We would like to thank Mr. Jeffrey A. Fox of the University of Dayton Research Institute for his prompt software support without which timely completion of this paper would not have been possible.

### References

- [1] Harmon, D. and Saff, C., "Metal Matrix Composites: Testing, Analysis, and Failure Modes," *Damage Initiation and Growth in Fiber Reinforced Metal Matrix Composites*, ASTM STP 1032, E. W. S. Johnson, Ed., American Society for Testing and Materials, Philadelphia, 1988, pp. 237-250.
- [2] Marshall, D. B., Cox, B. N., and Evans, A. G., "The Mechanics of Matrix Cracking in Brittle-Matrix Fiber Composites," *Acta Metallurgica*, Vol. 33, No. 11, 1985, pp. 2013-2021.
- [3] McCartney, L. N., "Mechanics of Matrix Cracking in Brittle-Matrix Fibre-Reinforced Composites," *Proceedings of the Royal Society, London*, Vol. A409, 1987, pp. 329-350.
- [4] Karpur, P., Matikas, T. E., Krishnamurthy, S., and Ashbaugh, N., "Ultrasound for Fiber Fragmentation Size Determination to Characterize Load Transfer Behavior of Matrix-Fiber Interface in Metal Matrix Composites," *Review of Progress in Quantitative NDE*, D. O. Thompson and D. E. Chimenti, Eds., La Jolla, CA, 19-24 July 1992, Vol. 12B, 1992, pp. 1507-1513.
- [5] Karpur, P., Matikas, T. E., and Krishnamurthy, S., "Matrix-Fiber Interface Characterization in Metal Matrix Composites Using Ultrasonic Imaging of Fiber Fragmentation," *Seventh Technical Conference on Composite Materials, Mechanics and Processing*, America Society of Composites, Pennsylvania State University, University Park, PA, Vol. 1, 1992, pp. 420-427.
- [6] Matikas, T. E. and Karpur, P., "Matrix-Fiber Interface Characterization in Metal Matrix Composites Using Ultrasonic Shear-Wave Back-Reflection Coefficient Technique," *Review of Progress in Quantitative NDE*, D. O. Thompson and D. E. Chimenti, Eds., La Jolla, CA, 19-24 July 1992, Vol. 12B, 1992, pp. 1515-1522.

- [7] Quate, C. F., Atalar, A., and Wickramasinghe, H. K., "Acoustic Microscopy with Mechanical Scanning—A Review," *Proceedings of the IEEE*, Vol. 67, Aug. 1979, pp. 1092–1114.
- [8] Lemons, R. A. and Quate, C. F., "A Scanning Acoustic Microscope," *IEEE Ultrasonics Symposium*, 1973, pp. 18–21.
- [9] Briggs, G. A. D., *An Introduction to Scanning Acoustic Microscopy*, Microscopy Handbooks, Oxford University Press, Royal Microscopical Society, Oxford, UK, Vol. 12, 1985.
- [10] Briggs, G. A. D., *Acoustic Microscopy*, Oxford University Press, Oxford, UK, 1992.
- [11] Lawrence, C. W., Briggs, G. A. D., Scruby, C. B., and Davies, J. R. R., "Acoustic Microscopy of Ceramic-Fibre Composites; Part I: Glass-Matrix Composites," *Journal of Materials Science*, Vol. 28, 1993, pp. 3635–3644.
- [12] Lawrence, C. W., Briggs, G. A. D., and Scruby, C. B., "Acoustic Microscopy of Ceramic-Fibre Composites; Part II: Glass-Ceramic-Matrix Composites," *Journal of Materials Science*, Vol. 28, 1993, pp. 3645–3652.
- [13] Lawrence, C. W., Briggs, G. A. D., and Scruby, C. B., "Acoustic Microscopy of Ceramic-Fibre Composites; Part III: Metal-Matrix Composites," *Journal of Materials Science*, Vol. 28, 1993, pp. 3653–3660.
- [14] Bertoni, H. L., "Rayleigh Waves in Scanning Acoustic Microscopy," *Rayleigh-Wave Theory and Application*, E. A. Ash and E. G. S. Paige, Eds., The Royal Institution, London, Vol. 2, 1985, pp. 274–290.
- [15] Liang, K. K., Kino, G. S., and Khuri-Yakub, B. T., "Material Characterization by the Inversion of  $V(z)$ ," *IEEE Transactions on Sonics and Ultrasonics*, Vol. SU-32, No. 2, 1985, pp. 213–224.
- [16] Jira, J. R. and Larsen, J. M., "Fatigue of Unidirectional SCS-6/Ti-24Al-11Nb Composite Containing a Circular Hole (Part II)," companion paper submitted to *Metallurgical Transactions A*, Carnegie Mellon University, Pittsburgh, PA (*Metallurgical Transactions*), 1993.
- [17] John, R., Jira, J. R., Larsen, J. M., and Ashbaugh, N. E., "Fatigue Crack Growth in Unidirectional SCS-6/Ti-24Al-11Nb Composite Containing a Circular Hole (Part II)," companion paper submitted to *Metallurgical Transactions A*, Carnegie Mellon University, Pittsburgh, PA (*Metallurgical Transactions*), 1993.
- [18] Blatt, D., Karpur, P., Stubbs, D. A., and Matikas, T. E., "Observations of Interfacial Damage in the Fiber Bridged Zone of a Titanium Matrix Composite," *Scripta Metallurgica et Materialia*, Vol. 29, 1993, pp. 851–856.
- [19] Buynak, C. F., Moran, T. J., and Martin, R. W., "Delamination and Crack Imaging in Graphite-Epoxy Composites," *Materials Evaluation*, Vol. 47, April 1989, pp. 438–447.
- [20] Blatt, D., John, R., and Coker, D., "Stress Intensity Factor and Compliance Solutions for a Single Edge Notched Specimen with Clamped Ends," submitted to *Engineering Fracture Mechanics*, 1993.
- [21] Krautkramer, J. and Krautkramer, H., *Ultrasonic Testing of Materials*, Springer-Verlag, New York, 1990.
- [22] Blatt, D., "Fatigue Crack Growth of Metal Matrix Composites Under Thermomechanical Loading." Ph.D. thesis, Purdue University, West Lafayette, IN, Dec. 1993.

## **Photocopy Rights**

Authorization to photocopy items for internal or personal use, or the internal or personal use of specific clients, is granted by the AMERICAN SOCIETY FOR TESTING AND MATERIALS for users registered with the Copyright Clearance Center (CCC) Transactional Reporting Service, provided that the base fee of \$2.50 per copy, plus \$0.50 per page is paid directly to CCC, 222 Rosewood Dr., Danvers, MA 01923; Phone: (508) 750-8400; Fax: (508) 750-4744. For those organizations that have been granted a photocopy license by CCC, a separate system of payment has been arranged. The fee code for users of the Transactional Reporting Service is 0-8031-2003-6 / 95 \$2.50 + .50.

## **Peer Review Policy**

Each paper published in this volume was evaluated by three peer reviewers. The authors addressed all of the reviewers' comments to the satisfaction of both the technical editor(s) and the ASTM Committee on Publications.

The quality of the papers in this publication reflects not only the obvious efforts of the authors and the technical editor(s), but also the work of these peer reviewers. The ASTM Committee on Publications acknowledges with appreciation their dedication and contribution to time and effort on behalf of ASTM.